Measurement of the K_{e2}^+ Branching Ratio*

D. R. BOWEN, A. K. MANN, AND W. K. MCFARLANE
Department of Physics, University of Pennslyvania, Philadelphia, Pennsylvania

AND

A. D. FRANKLIN, E. B. HUGHES, R. L. IMLAY, G. K. O'NEILL, AND D. H. READING
Princeton University, Princeton, New Jersey

(Received 19 September 1966)

The K_{e2}^+ branching ratio has been measured in a spark-chamber and counter experiment at the Princeton-Pennsylvania accelerator. A K^+ beam which yielded an average of 500 stopped, identified K^+ mesons per second was used. Particles which left the stopping region approximately at right angles to the incident beam passed through a series of six thin-plate chambers situated in a 7.5-kG magnetic field which permitted measurement of the particle momentum with a standard deviation of 1.9%. Positrons were identified by a threshold gas Čerenkov counter placed behind the magnetic field. A thick-plate spark chamber was placed behind the Čerenkov counter to permit observation of a particle emerging from that counter and measurement of the particle's total range. The time interval between the K^+ stop and decay was recorded for each event. Discrimination against background events, arising principally from the $K\mu_2^+$ decay mode, was provided by selection criteria on momentum, range, the time between the K^+ stop and decay, and by a requirement that the measured position of the track at the entrance to the thick-plate chamber match the extrapolated momentum chamber track. After applying these criteria, we obtain a total of seven events in the momentum interval 242–252 MeV/c in which positrons from K_{e2}^+ should fall, with 2.8 of these events estimated to be background. This gives a K_{e2}^+ branching ratio of $(2.1_{-1.3}^{+1.8})\times10^{-5}$, in agreement with the prediction of $V-A$ theory, which, including a radiative correction, is 1.44×10^{-5}.

INTRODUCTION

A SPARK-chamber and counter experiment has been performed at the Princeton-Pennsylvania accelerator (PPA) to measure the branching ratio for $K^+\to e^++\nu$ (K_{e2}^+ decay). The pure leptonic decays of the charged π and K mesons provide stringent tests of the $V-A$ theory[1,2] of weak interactions. Thus the agreement between the predicted ratio of the rates for $\pi^+\to e^++\nu$ and $\pi^+\to\mu^++\nu$ and the observed ratio[3] represents one of the triumphs of present $V-A$ theory. The analogous decays for the kaon, $K^+\to e^++\nu$ and $K^+\to\mu^++\nu$, involve a change of strangeness and much higher relative momenta of the leptons. Assuming the kaon to be pseudoscalar, one obtains for the ratio, $R=\text{Rate}(K_{e2}^+)/\text{Rate}(K_{\mu2}^+)$,

$$R=\frac{[1-(m_e^2/m_K^2)]^2[f_P-(m_e/m_K)f_A]^2}{[1-(m_\mu^2/m_K^2)]^2[f_P-(m_\mu/m_K)f_A]^2},$$

where f_A and f_P are the axial-vector and pseudoscalar coupling constants, respectively. Pure axial-vector coupling predicts $R=2.6\times10^{-5}$ (without radiative corrections), while pure pseudoscalar coupling predicts $R=1.02$. Adding a small admixture of pseudoscalar coupling to a pure axial-vector interaction greatly alters the calculated K_{e2}^+ rate. For example, if the constants f_P and f_A are in the ratio 10^{-3}, the K_{e2}^+ rate is about four times the value for pure f_A. The best previous measurement of the K_{e2}^+ branching ratio[4] gives an upper limit for R of 2.6×10^{-3} which is a factor of 100 higher than the predicted $V-A$ ratio. Thus even a rough measurement of the K_{e2}^+ rate can provide an additional test of the applicability of $V-A$ theory to strangeness nonconserving weak interactions and give a stringent test of the presence of any P amplitude in the weak interaction of the kaon.

EXPERIMENTAL APPARATUS

A positive unseparated beam was obtained at the PPA with the beam transport system shown in Fig. 1. This double focusing system is very similar to one used in a previous experiment.[5] It differs in three major features: (1) the momentum bite here was increased from 7% to 13% full width at half maximum (FWHM) around the central momentum, 530 MeV/c, (2) the beam length was shortened from 8.8 to 7.2m, and (3) off-axis bending in the quadrupoles was eliminated. This beam yielded an average of 500 stopped, identified K^+ mesons per second, averaged over several months,

* Work performed under the auspices of the U. S. Atomic Energy Commission.

[1] R. P. Feynman and M. Gell-Mann, Phys. Rev. **109**, 193 (1958).

[2] E. C. G. Sudarshan and R. E. Marshak, in *Proceedings of the Padua-Venice Conference on Fundamental Particles, Padua 1957*, (Societa Italiana di Fisica, Bologna, Italy, 1957), p. V-14; Phys. Rev. **109**, 1860 (1958).

[3] T. Fazzini, G. Fidecaro, A. W. Merrison, H. Paul, and A. V. Tollestrup, Phys. Rev. Letters **1**, 247 (1958); G. Impeduglia, R. Plano, A. Prodell, N. Samios, M. Schwartz, and J. Steinberger, *ibid.* **1**, 249 (1958); H. L. Anderson, T. Fuji, R. H. Miller, and L. Tau, Phys. Rev. **119**, 2050 (1960); E. Di Capna, R. Garland, L. Pondrom, and A. Strelzoff, *ibid.* **133**, B1333 (1964).

[4] G. Borreani, G. Rinaudo, and A. E. Werbrouck, Phys. Letters **12**, 123 (1964). This paper quotes an upper limit for the K_{e2}^+ branching ratio of 1.6×10^{-3}, which corresponds to $R=2.6\times10^{-3}$.

[5] L. B. Auerbach, J. MacG. Dobbs, A. K. Mann, W. K. McFarlane, D. H. White, R. Cester, P. T. Eschstruth, G. K. O'Neill, and D. Yount, Phys. Rev. (to be published); R. Cester, P. T. Eschstruth, G. K. O'Neill, B. Quassiati, D. Yount, J. M. Dobbs, A. K. Mann, W. K. McFarlane, and D. H. White, Phys. Letters **21**, 343 (1966).

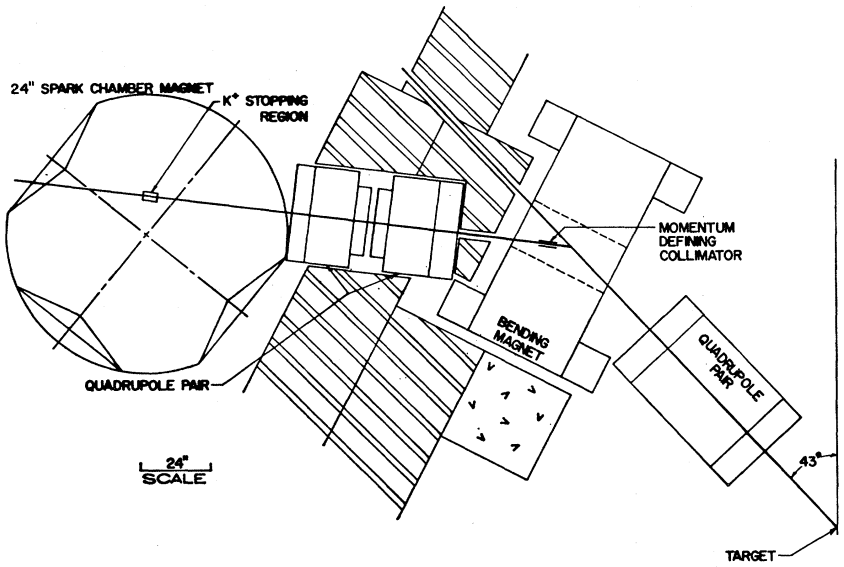

FIG. 1. The beam-transport system.

with the detection system shown in Fig. 2. A maximum rate of 800 kaons/sec was obtained for periods of several hours.

The kaons were identified by range and time of flight. A total of 6.7 cm of copper placed in the beam served to stop the kaons in the stopping region C_3, which was a scintillation counter 5.1-cm high $\times$3.8-cm wide $\times$12.7-cm long. A stopped-beam particle was identified by the counter coincidence $C_1C_2C_3\bar{C}_4$. The copper also eliminated almost all protons in the beam. Approximately 80% of the pions were eliminated by the veto counter C_4. Further discrimination against pions was made by using the rf structure of the internal beam. The internal beam of the PPA retains its bunched structure and phase relative to the driving rf waveform as it strikes the internal target. The proton bunches are about 1.5-nsec wide and 34-nsec apart. Thus a signal derived from the synchrotron rf system may be used to measure times of flight over the beam length (with ambiguities of 34 nsec). Figure 3 shows the number of beam and of stopped particles as a function of the delay of the rf signal. The pions and kaons are separated by 8 nsec. A narrow coincidence (3-nsec wide) ($C_1C_2C_3\bar{C}_4$ and rf) identified stopped K^+ mesons with a background of less than 5% pions.

Particles which left the stopping region approximately at right angles to the incident beam passed through a series of six thin-plate spark chambers situated in a

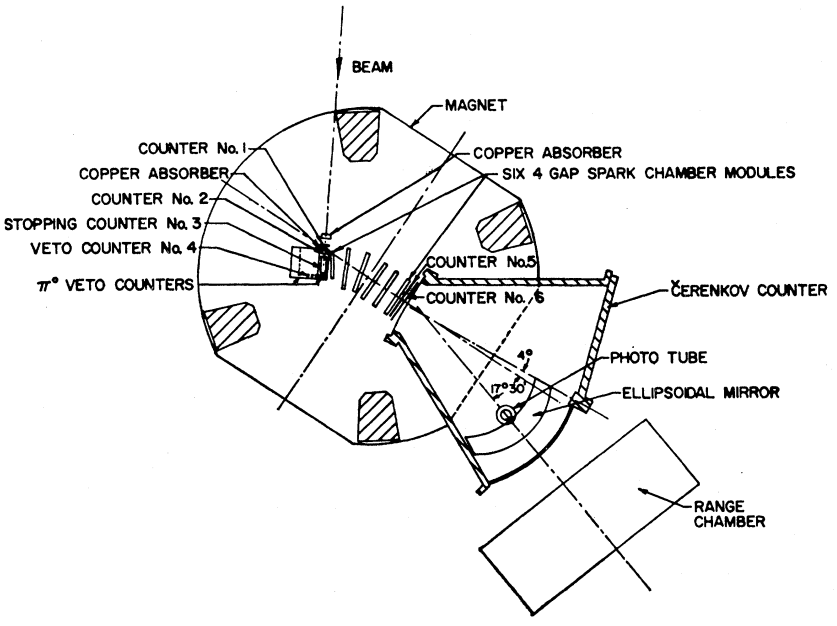

FIG. 2. Details of the experimental arrangement.

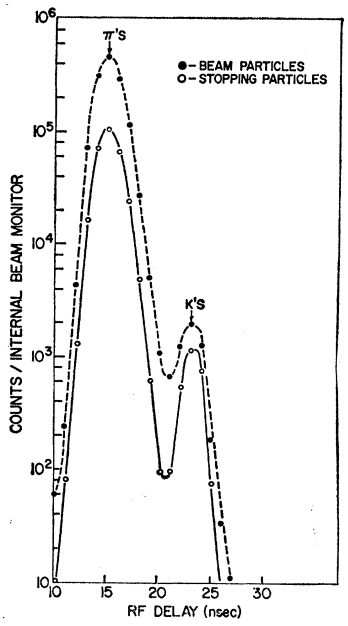

FIG. 3. Distribution in time of particles reaching the K^+ stopping region.

7.5-kG magnetic field about 2-ft long. This permitted measurement of the particle momentum with a standard deviation of 1.9%. The momentum resolution was limited by individual spark scatter and by multiple scattering in the 180 mg/cm² of aluminum in the spark chambers.

Decay particles were detected by a telescope consisting of two scintillation counters (C_5 and C_6) and a threshold gas Čerenkov counter set to detect only high-momentum positrons, situated behind the magnetic field. This Čerenkov counter has been described in detail elsewhere.[6] It had a measured efficiency of greater than 99% for 250-MeV/c positrons passing through the center of the front and rear windows of the counter. The efficiency fell off to 95% for positrons passing through the extreme outside edge of the rear window. The counter had an efficiency of approximately 0.38% for other particles of comparable momentum. For this experiment only half the Čerenkov counter was necessary and this fixed the relative solid angle at 0.74×10^{-2}.

A distribution of time intervals between the stopping K^+ telescope ($C_1C_2C_3\bar{C}_4$ and rf) and the decay particle pulse (determined from counters C_5 and C_6), is shown in Fig. 4. The two peaks are associated with pions from the same and the succeeding rf bunch as the kaon, and the kaon lifetime is clearly shown. The smaller peak of pions in the same rf bunch as the kaon is due to the fact that a pion in the same rf bunch as the kaon will, in general, veto the kaon. A gate was used to eliminate this pion background as indicated on Fig. 4.

A thick-plate range chamber was placed behind the Čerenkov counter to permit observation of the particles emerging from that counter and measurement of their total range. The total thickness of the chamber was 80 g/cm² of aluminum, which was enough to stop all particles resulting from the decay of the K^+ meson. For much of the experiment counters which detected gamma rays were used to suppress events accompanied by a π^0, e.g., $K^+\rightarrow e^++\pi^0+\nu$. These counters were lead-scintillator sandwiches located above and below the K^+ stopping region, and reduced K_{e3}^+ events by a factor of roughly two. The spark chambers were triggered by a coincidence between a stopped K^+ meson and a decay positron, with the additional requirement of no detected gamma ray. The time between the K^+ stop and decay was recorded for each event.

DATA ANALYSIS

Calculation of Backgrounds

The positron from K_{e2}^+ decay has a momentum of 246.9 MeV/c in the kaon center-of-mass (c.m.) system. This momentum is higher than that of any other direct decay product of the K^+ meson, with the nearest competitor being the 235.6-MeV/c muon from $K_{\mu2}^+$. The principal sources of high-momentum positrons, which form a background to the real K_{e2}^+ events are

(1) $K^+\rightarrow e^++\pi^0+\nu$ with a maximum positron momentum of 228 MeV/c and a branching ratio of about 5%, and

(2) $K^+\rightarrow\mu^++\nu$ followed by $\mu^+\rightarrow e^++\nu+\bar{\nu}$ with a maximum positron momentum of 246.9 MeV/c and a branching ratio of approximately 1.2×10^{-4}/ft of muon path.

With an experimental momentum resolution of 1.9% the contribution of positrons from K_{e3}^+ decays at rest in the K_{e2}^+ momentum interval, 242–252 MeV/c, is

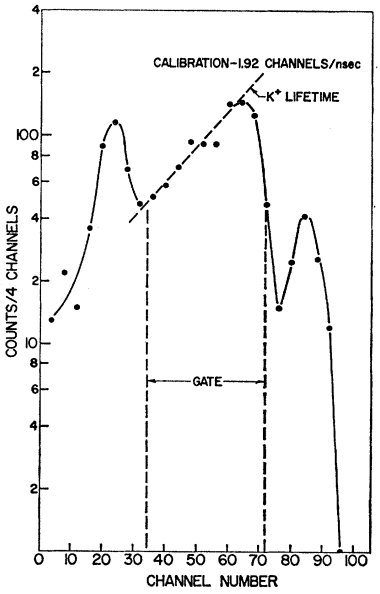

FIG. 4. Time distribution between a stopping K^+ pulse and a decay particle pulse.

[6] J. MacG. Dobbs, W. K. McFarlane, and D. Yount, Princeton-Pennsylvania Accelerator Report, PPAD-586E (unpublished); Nucl. Instrs. Methods (to be published).

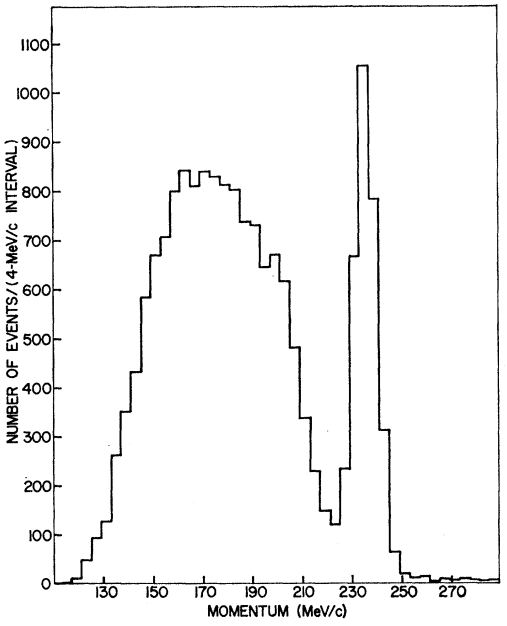

FIG. 5. Momentum distribution of all K^+ decay events obtained with the Čerenkov counter in triggering logic.

less than 5% of the K_{e2}^+ rate predicted by $V-A$ theory. K_{e3}^+ events from K^+ decays in flight may also contribute to the background; such events can be completely excluded, however, by eliminating all "prompt" events from the distribution of time intervals between the stopping-K^+ pulse and the decay-positron pulse, as discussed below in detail.

To consider the background due to decays in flight of muons from $K_{\mu 2}^+$ decay, we divide the experimental apparatus, shown in Fig. 2, into four regions: (1) 15 cm from the K^+ stopping region to the entrance to the momentum chamber, (2) the 60-cm length of the momentum chamber, (3) the 137-cm length from the end of the momentum chamber to the end of the Čerenkov counter, and (4) 76 cm beyond the Čerenkov counter.

In the 15-cm region (1) between the stopping region and the momentum chamber we calculate that the number of muon-decay positrons with momentum greater than 235 MeV/c is less than 1% of the K_{e2}^+ rate predicted by $V-A$ theory. In the 60 cm of the momentum chamber (region 2) we calculate that the number of decay positrons with laboratory angles of less than 10° with respect to the muon flight path and momentum greater than 225 MeV/c is less than 5% of the expected K_{e2}^+ rate. These limits on momentum and angle are well within our experimental resolution.

In the muon c.m. system the distribution of decay positrons as a function of angle and energy is, for muons from $K_{\mu 2}^+$ decay, given by

$$w(E)dE\,d\cos\Theta=[(3-2E)+\cos\Theta(1-2E)]E^2dE\,d\cos\Theta,$$

where E is measured relative to the maximum possible positron energy, 0.5 m_μ, and Θ is measured relative to the muon momentum (antiparallel to the muon spin). When we transform to the laboratory system we note that the positron is usually emitted at large angles to the muon path and with a widely different momentum, with high momentum positrons suppressed. We calculate the background expected due to muon decays in the Čerenkov counter (region 3) in the following manner. A Monte Carlo calculated simulates muon decays using the distribution given above. The efficiency of the Čerenkov counter as a function of position and angle of the decay positron is approximately given by a function of the distance of the extrapolated positron path from the Čerenkov counter axis at the K^+ stopping region. This function is unity from 0 to 15 cm and falls linearly to zero from 15 to 30 cm. We further require that the decay positron track agree with the original muon path to within ±8 cm in the horizontal direction and ±6 cm in the vertical direction at the entrance to the range chamber. This requirement we also use to eliminate background from muon decays and it is discussed in greater detail below. The Monte Carlo calculation subject to these requirements gives a background of approximately 75% of the expected K_{e2}^+ rate. It should be emphasized, however, that these muon decays occur after the momentum chamber and have therefore a measured momentum appropriate to that of muons from $K_{\mu 2}^+$ decay (235.6 MeV/c). Our momentum resolution reduces this background to approximately 10% of the expected K_{e2}^+ rate in the K_{e2}^+ momentum region, 242–252 MeV/c.

Muon decays which occur after the Čerenkov counter (region 4) will give rise to background events only if the decay is in accidental coincidence with a noise pulse in the Čerenkov counter. From the observed counting rate in the Čerenkov counter we obtain a background of approximately 10% of the expected K_{e2}^+ rate from this source. Since these events will also have a $K_{\mu 2}^+$ momentum, the momentum resolution reduces this background to less than 2% of the K_{e2}^+ rate in the K_{e2}^+ momentum region.

The above calculations give rise to a total background of approximately 15% of the expected K_{e2}^+ rate in the K_{e2}^+ momentum region. There are other sources of background, due to experimental effects, which are not calculable *a priori*, and which are discussed in detail in the next section.

Reduction of Data

In Fig. 5 the momentum distribution of 16 965 events obtained with the Čerenkov counter in the triggering logic is shown. These events satisfy the following criteria: (1) The track emerged from the K^+ stopping region. (2) The track passed through both the front and rear windows of the Čerenkov counter. (3) A track was observed to traverse at least 3 plates in the thick-plate spark chamber. Approximately 64% of all measured events passed the first two criteria. Table I shows

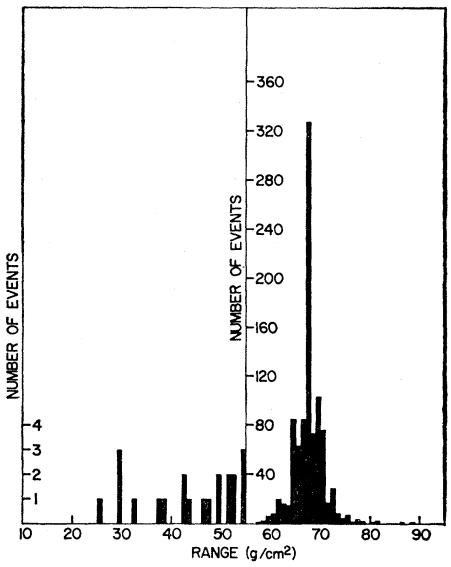

FIG. 6. Range spectrum for $K_{\mu 2}^+$ muons.

the effect of the selection criteria on the original event sample.

The K_{e3}^+ spectrum falls off rapidly below 160-MeV/c momentum because positrons of lower momentum are deflected by the magnetic field and miss the Čerenkov counter. The 2914 events in the peak at 236 MeV/c and about 675 events in the bump at 205 MeV/c are due to accidental coincidences between accelerator-produced background in the Čerenkov counter and muons and pions from $K_{\mu 2}^+$ and $K_{\mu 2}^+$ decays, respectively. The $K_{\mu 2}^+$ peak has been reduced by a factor of 260 by the presence of the Čerenkov counter, and the $K_{\pi 2}^+$ peak by an additional factor of 1.47 due to the π° veto counters. We have calibrated our momentum scale using the known momentum of the $K_{\mu 2}^+$ peak. The momentum resolution of 1.9% was found by fitting a Gaussian to the $K_{\mu 2}^+$ peak; part of this width (about 16%) arises from energy loss in the target.

To reduce the enormous $K_{\mu 2}^+$ peak in Fig. 5, we apply a range criterion. We have defined range as the total path length in the thick-plate spark chamber before the first "interaction" (if any) occurs. An interaction is defined by a gap of three or more sparks in the track or by a vee in which both emerging tracks have at least two sparks. The range spectrum for a sample of muons from $K_{\mu 2}^+$ decay, selected by having a measured momentum between 231 MeV/c and 241 MeV/c, and without the Čerenkov counter in the triggering logic, is shown in Fig. 6. The muons have a mean measured range of 67 g/cm² of aluminum with a straggle of about 4 g/cm². High-momentum positrons do not have a well-defined range, but have an apparent range of roughly one radiation length, about 27 g/cm² of aluminum. A range spectrum for a sample of events with momentum between 212 MeV/c and 227 MeV/c, with the Čerenkov counter in the logic, mainly K_{e3}^+ events, is shown in Fig. 7, which has been corrected for a $K_{\mu 2}^+$ muon contamination of about 7%. The percentage of K_{e3}^+ events in the interval 212 to 227 MeV/c and with effective range less than a given value is shown in Table II.

We have made a range cut at 45 g/cm² to minimize background due to $K_{\mu 2}^+$ events while preserving a large and known fraction of the high momentum positron events (see Figs. 6 and 7). Figure 8 shows the effect of this range cut for events with momentum greater

TABLE I. The effect of the experimental-geometry criteria is shown. The large percentage of events eliminated by the stopping-region (vertical) criterion is due to the presence of counters and light pipes above and below the stopping region in which K^+ mesons scattered out of the useful stopping region can also stop.

Criterion	Percentage of events eliminated
Stopping region (horizontal)	6.0
Stopping region (vertical)	22.5
Čerenkov counter entrance (horizontal)	3.1
Čerenkov counter entrance (vertical)	4.1
Čerenkov counter exit (horizontal)	10.9
Čerenkov counter exit (vertical)	2.8

TABLE II. Range distribution of positrons from K_{e3}^+ in the momentum interval 212–227 MeV/c.

Range (g/cm²)	% of events with smaller range
40	45.6±2.1
45	51.9±2.1
50	59.2±2.1
55	68.8±1.9

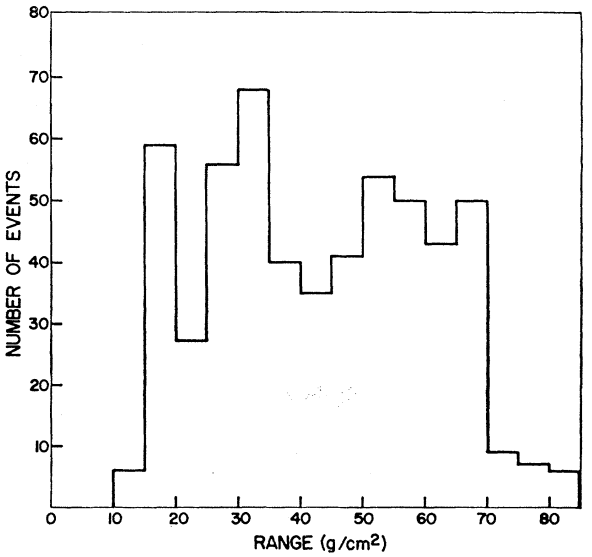

FIG. 7. Range spectrum for K_{e3}^+ positrons with momentum between 212 and 227 MeV/c.

than 212 MeV/c. All events with momentum greater than 212 MeV/c and range less than 45 g/cm^2 were inspected for evidence of equipment failures or bad range chamber pictures. Such events, which constituted 9% of the events above 212 MeV/c, were excluded from Fig. 8. We see that the peak at 236 MeV/c is reduced by a factor of approximately sixteen, while the region between 212 and 227 MeV/c is depleted by a factor of about 2. Note that in Fig. 6 only 1% of the $K_{\mu 2}^+$ events (10 out of 978) have a measured range of less than 45 g/cm^2. We reduce the peak at 236 MeV/c in Fig. 8 by a factor of 16 rather than 100 because of the presence of $K_{\mu 2}^+$ muons which have decayed in flight. The 1% of $K_{\mu 2}^+$ muons of range less than 45 g/cm^2 is too large to be accounted for by range straggling and is due to occasional failure of the range chamber to operate properly. These apparatus failures give rise to a background approximately equal to the expected K_{e2}^+ rate, but such events have a $K_{\mu 2}^+$ momentum and the background from this source in the K_{e2}^+ region is depressed to approximately 15% of the expected K_{e2}^+ rate, i.e., an amount equal to the total background calculated in the previous section.

As stated above, positrons resulting from $K_{\mu 2}^+$ muons which decay in flight are usually emitted at wide angles to the muon path. Thus the background due to muon decays in flight occurring between the end of the momentum chamber and the exit of the Čerenkov counter (region 3 noted above) can be reduced by comparing the measured position of the track entering the range chamber with the position predicted by extrapolating the track observed in the momentum chamber. The accuracy of this comparison is limited by multiple scattering and by errors in extrapolating the momentum chamber track. Figures 9 and 10 show the distributions in the difference between the observed and extrapolated track positions in the horizontal (ΔX) and vertical (ΔY) directions, for events with momentum between 207 MeV/c and 227 MeV/c and range less than 45 g/cm^2, mainly K_{e3}^+ positrons. A fiducial area was chosen, as indicated on the figures, with accepted intervals -6 to $+10$ cm in the horizontal direction and -7 to $+6$ cm in the vertical direction. These intervals allowed approximately 54% of the events in Fig. 8 to enter the final sample. The width of these distributions is twice the width expected from multiple scattering and is due to errors in extrapolating the long particle path through the fringe field of the magnet. This accounts for the greater width of the horizontal distribution. The center of the horizontal distribution varied slightly with

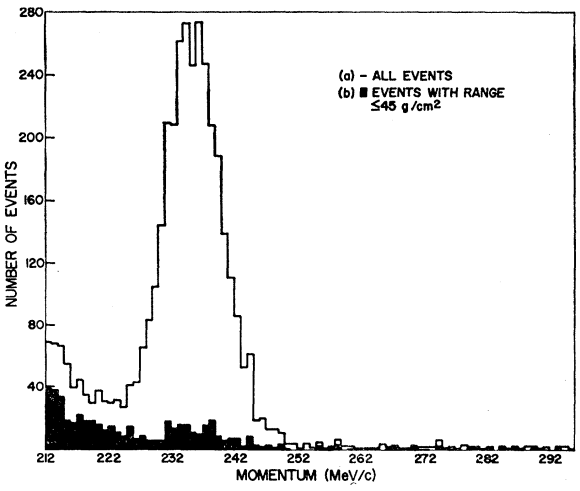

FIG. 8. Momentum spectrum of particles with $p \geq 212$ MeV/c: (a) all events and (b) events with range ≤ 45 g/cm^2.

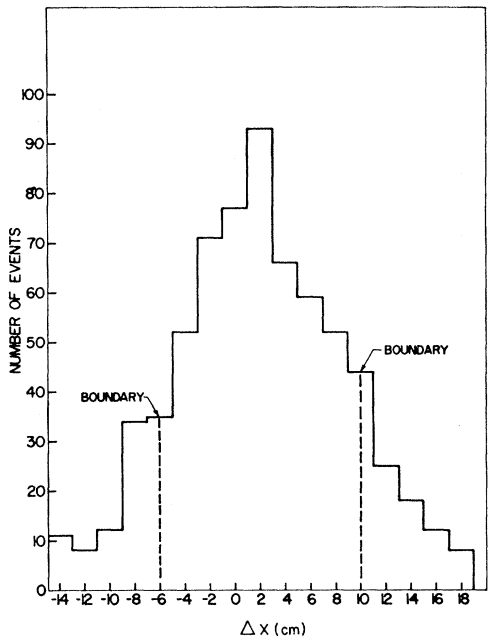

FIG. 9. Distribution of the difference in the horizontal direction (ΔX) between the extrapolated momentum chamber track and the measured range chamber track for particles with momentum between 207 and 227 MeV/c.

TABLE III. Effect of the track-matching criterion for events with range less than 45 g/cm^2. The number of events in the momentum regions of interest does not change significantly for small variations of the fiducial area. The accepted intervals were -6 to $+10$ cm in the horizontal direction and -7 to $+6$ cm in the vertical direction in the momentum interval 212–227 MeV/c. Changes in the accepted intervals were made in both the horizontal and vertical directions.

Momentum region (MeV/c)	Fiducial area: None	Accepted intervals	Accepted intervals increased by 2 cm	Accepted intervals decreased by 2 cm
$P \leq 212$	525	214	240	184
K_{e3}^+ (212–228)	297	161	177	143
$K_{\mu 2}^+$ (231–241)	134	28	35	20
K_{e2}^+ (242–252)	33	13	13	11
$P \geq 252$	36	5	6	4

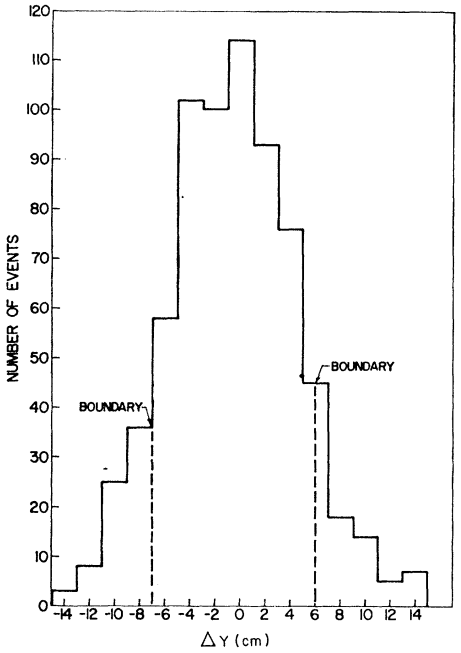

FIG. 10. Distribution of the difference in the vertical direction (ΔY) between the extrapolated momentum chamber track and the measured range chamber track for particles with momentum between 207 and 227 MeV/c.

momentum and we have adjusted the fiducial areas appropriately to take this into account. At a momentum of 220 MeV/c, a 15% change in momentum resulted in a 2-cm shift of the center of the distribution. This variation is only 12.5% of the total width of the accepted interval and is probably due to mismatching between the central magnetic field and the less accurately known fringe field. We see in Table III that the number of events in the several momentum regions of interest does not change significantly with small variations of the fiducial area.

The application of this track-matching criterion preferentially reduces events in the $K_{\mu 2}^+$ region and in the region above the K_{e2}^+ momentum interval. Figure 11 shows the effect of this track matching criterion on events with range less than 45 g/cm^2 and momentum greater than 212 MeV/c. To guard against muon decays in flight and large multiple scattering in the momentum chamber which would result in an incorrect momentum, we required that a measured track show a good fit to the polynomial used to approximate the track in the momentum chamber and also that a track have a relatively constant momentum along its entire path. A total of only 14 events were eliminated by these fitting criteria, none of which were in the K_{e2}^+ region. The effect of these criteria is included in Fig. 11.

Figure 12 shows the distribution of time intervals between the stopping-K^+ pulse and the decay-positron pulse for all events. Examination of $K_{\mu 2}^+$ muons indicated the presence of a small prompt peak due to K^+ meson decays in flight. This peak had a base width of about 2 nsec. To eliminate such prompt events we have made a cut at 2.75 nsec from the half-height of the leading edge of the time spectrum. The effect of this criterion on events with momentum greater than 212 MeV/c which satisfy the range- and track-matching criteria is shown in Fig. 13; it eliminates 15% of the K_{e3}^+ events and 46% of the nominal K_{e2}^+ events. We consider as the final sample those events which satisfy all criteria: momentum greater than 212 MeV/c, range ≤ 45 g/cm^2, track matching, and kaon decay time. The quantitative conclusions discussed in the next section are not significantly altered by the inclusion of events with ranges between 45 and 55 g/cm^2, or by reasonable changes in the track-matching criterion (see Table III) or by reasonable changes in the kaon decay-time criterion.

RESULTS

We define four momentum regions in the final sample of events: (1) K_{e3}^+, 212–228 MeV/c; (2) $K_{\mu 2}^+$, 231–241 MeV/c; (3) K_{e2}^+, 242–252 MeV/c; and (4) background, momentum greater than 252 MeV/c. In the K_{e2}^+ region (3) there are seven events. We calculate the background in this region in the following manner. The flat background (region 4) has 2 events in 30 MeV/c and hence we expect 0.67 ± 0.5 events per 10-MeV/c interval. In the $K_{\mu 2}^+$ region (2) there are 22 events. We subtract 0.67 events due to flat background, 1.5 events due to K_{e3}^+ events, and 0.7 due to K_{e2}^+, leaving a total of 19.1 ± 4.8 $K_{\mu 2}^+$ events. Since we look only in a limited momentum region (10 MeV/c) with a momentum resolution of 1.9% we multiply the number of $K_{\mu 2}^+$ events by 1.38 giving a final total of (26.3 ± 6.6) $K_{\mu 2}^+$ events. From this and the above momentum resolution we obtain (2.1 ± 0.5) $K_{\mu 2}^+$ events in the K_{e2}^+ region. Thus the background in the K_{e2}^+ region is (2.1 ± 0.5) events from $K_{\mu 2}^+$ plus (0.67 ± 0.5) events from the flat background.

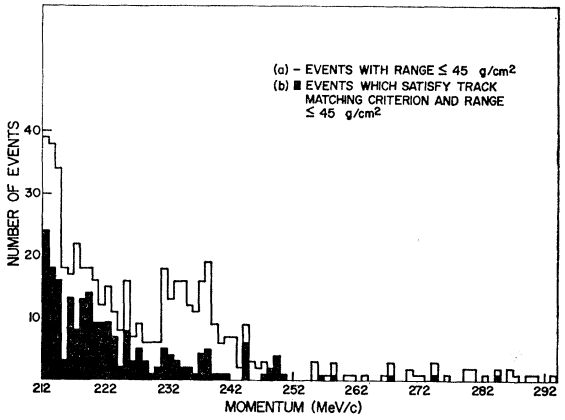

FIG. 11. Momentum spectrum of particles with $p \geq 212$ MeV/c and range ≤ 45 g/cm^2: (a) all events and (b) events satisfying the track-matching criterion.

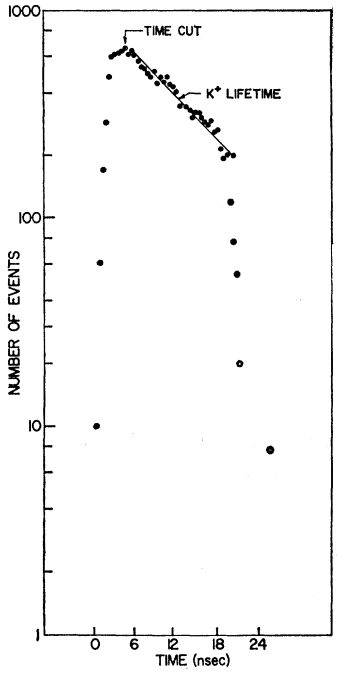

FIG. 12. Distribution of time intervals between the stopping K^+ pulse and the decay-particle pulse.

We are left with $4.2_{-2.6}^{+3.7}$ K_{e2}^+ events and correction for the limited momentum interval gives a final total of $6.0_{-3.7}^{+5.2}$ K_{e2}^+ events. Note that the probability of observing 7 background events in the region (3) where we expect 2.8 background events is 1.6%.

In order to calculate a branching ratio we must normalize the K_{e2}^+ events to a more abundant decay mode. This has been done in two different ways. The first method uses the 136 events in the K_{e3}^+ region (1) of the final sample. We correct the number of K_{e3}^+ events for background due to Dalitz pairs (−3%), for some $K_{\pi 2}^+$ events which are also found in this momentum region (−9%), for events lost by radiative K_{e3}^+ decay (+5%), for the fact that the solid angle in this momentum region is 4% lower than that in the K_{e2}^+ region, and for a small differential dependence on range of the K_{e3}^+ and K_{e2}^+ detection efficiences (4%). We assume that the loss of events due to positron bremsstrahlung is the same for K_{e2}^+ and these high-momentum K_{e3}^+ events. This yields a corrected total of 126.5 K_{e3}^+ events. Since the π° veto counters eliminated 32% of the K_{e3}^+ events, averaged over the entire experiment, we obtain a final total of 185.3 K_{e3}^+ events in region (1). This momentum region corresponds to 1.27% of the total K_{e3}^+ spectrum calculated using a pure vector spectrum.[5] For a K_{e3}^+ branching ratio[5] of (4.93±0.13)% we obtain a branching ratio per K_{e2}^+ event of $(3.38\pm0.3)\times10^{-6}$. Multiplying by the $6.0_{-3.7}^{+5.2}$ observed K_{e2}^+ events, we find a K_{e2}^+ branching ratio of $(2.0_{-1.2}^{+1.8})\times10^{-5}$.

The second method uses the total sample of 16 965 events of Fig. 4. There are approximately 2914 $K_{\mu 2}^+$ events, 675 $K_{\pi 2}^+$ events, and 677 background events as determined from the region above the $K_{\pi 2}^+$ peak, leaving a total of 12 699 K_{e3}^+ events. The spectrum fraction has been calculated using a Monte Carlo calculation, which yielded 0.30±0.03. Including the effect of the π° veto counters and the decay time criterion the total is $(51.2\pm5.1)\times10^3$ K_{e3}^+ events. These events have not been subjected to the range- or track-matching criteria. It was simpler to remove the effect of these momentum-dependent criteria in the K_{e2}^+ sample rather than in the total number of K_{e3}^+ events. The percentage of events in the K_{e2}^+ region (3) passing these criteria has been estimated above and is as follows: (1) range (48±2)%, (2) track matching (54.2±2.8)%. Dividing by these ratios to estimate the effective number of K_{e2}^+ events under these conditions gives 22.9_{-14}^{+20} K_{e2}^+ events and normalizing to the total K_{e3}^+ event sample gives a K_{e2}^+ branching ratio of $(2.2_{-1.4}^{+1.9})\times10^{-5}$. A similar calculation using events without applying any time selection criterion gives a K_{e2}^+ branching ratio of $(3.5\pm1.4)\times10^{-5}$ normalized to the selected upper end of the K_{e3}^+ spectrum and $(3.8\pm1.6)\times10^{-5}$ normalized to all K_{e3}^+ events. We choose as the best value for the K_{e2}^+ branching ratio the mean of the two ratios calculated with the time selection criterion and obtain $R(K_{e2}^+/K^+)=(2.1_{-1.3}^{+1.8})\times10^{-5}$.

CONCLUSIONS

The measured value of the K_{e2}^+ branching ratio,

$$R(K_{e2}^+/K^+)=(2.1_{-1.3}^{+1.8})\times10^{-5},$$

is in agreement with the result, 1.44×10^{-5}, predicted by the $V-A$ theory. The theoretical value includes radiative corrections[7] corresponding to our experimental energy resolution. Based on a value of the branching ratio 2 standard deviations greater than the measured value, we obtain an upper limit of 3.0×10^{-3} for the ratio of the pseudoscalar to the axial-vector amplitude in the leptonic decays of charged kaons.

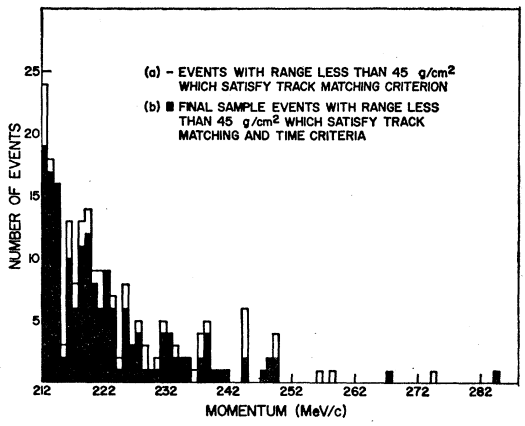

FIG. 13. Momentum spectrum of particles with $p\geq212$ MeV/c, range ≤45 g/cm² and satisfying the track matching criterion: (a) all events and (b) events with K^+ decay time ≥2.75 nsec.

[7] S. M. Berman, Phys. Rev. Letters **1**, 468 (1958).

ACKNOWLEDGMENTS

We would like to thank the staff of the Princeton-Pennsylvania Accelerator for their unfailing cooperation. We would also like to thank Kenneth Wright and Howard Crothamel for their aid in the construction of the mechanical apparatus and Bart Gibbs and Edward Mayer for their help in the construction of the electrical equipment. Thanks are also due to our scanners supervised by Miss Shirley Markowitch, Mrs. Y. Kim and Walter Grant, for performing so well the arduous task of scanning and measuring the film. L. B. Auerbach, R. Cester, J. MacG. Dobbs, P. T. Eschstruth and E. Miller provided helpful discussions. Most of the calculations were performed at the Princeton University Computing Center.

PHYSICAL REVIEW VOLUME 154, NUMBER 5 25 FEBRUARY 1967

Effect of a Castillejo-Dalitz-Dyson Pole in the πN $I=\frac{1}{2}$, $J=\frac{1}{2}^+$ Amplitude*

BIDHANCHANDRA I. SHETH† AND ARNOLD TUBIS
Department of Physics, Purdue University, Lafayette, Indiana
(Received 30 September 1966)

Recent phase-shift analyses of the $I=\frac{1}{2}$, $J=\frac{1}{2}^+$ πN amplitude imply that the real part of the phase shift changes sign at about 150-MeV pion lab kinetic energy and either passes through 90° or reaches a maximum slightly below 90° at about 600 MeV. These features of the phase shift strongly contradict the predictions of dispersion-theory calculations of the nucleon mass, which generally yield a negative phase shift decreasing with increasing energy. We assume that the observed phase-shift behavior is due to multichannel-coupling effects which can be accounted for in a single-channel calculation only by including a Castillejo-Dalitz-Dyson pole. A previous determination of the nucleon mass, m, and coupling with pions, $g^2/4\pi$, based on the assumed knowledge of the πN $I=\frac{3}{2}$, $J=\frac{3}{2}^+$ (N^*) resonance parameters, is repeated with the inclusion of a CDD pole. A variant of the Balázs method is used. The CDD pole parameters are determined so as to give the phase-shift behavior mentioned above. The Balázs-pole residues are determined by requiring crossing symmetry in a form relating the πN amplitude on the nearby left-hand cut to physical πN scattering. We find $m=0.97$ in units of the physical nucleon mass; $g^2/4\pi=10.5$; and a πN $I=\frac{1}{2}$, $J=\frac{1}{2}^+$ scattering length between about -0.038 and -0.048 (in units of the cube of the pion Compton wavelength), depending on the assumed energy at which the phase shift changes sign. These parameters appear to be very insensitive to the choice of Balázs-pole positions.

I. INTRODUCTION

In a recent paper, Doolen, Kanki, and Tubis,[1] hereafter referred to as DKT, have used a variant of the Balázs method[2] to calculate the nucleon mass m and coupling with pions $g^2/4\pi$ from a knowledge of the resonant πN scattering in the $I=\frac{3}{2}$, $J=\frac{3}{2}^+$ state. They circumvented the matching-point ambiguity associated with the Balázs method by requiring a certain crossing relation to be satisfied over a finite region where it is fairly certain that all important contributions to the relation are taken into account. They obtained $m=1.03$ in units of physical nucleon mass and $g^2/4\pi=18.6$, in fairly good agreement with the experimental values, $m=1$ and $g^2/4\pi=15.1\pm0.6$.[3]

However, their calculated πN $I=\frac{1}{2}$, $J=\frac{1}{2}^+$ phase shift (δ_{11}) is negative and decreases with increasing energy. This behavior is in strong contradiction with recent phase-shift analyses[4–9] which imply that the real part of the phase shift changes sign at about 150-MeV pion lab kinetic energy[4,5] and either passes through 90°[4–7] or reaches a maximum slightly below[8] 90° at about 600 MeV.[10] The behavior at ~600 MeV is usually referred to as the "Roper resonance."

* This work supported in part by the U. S. Air Force Office of Scientific Research, Office of Aerospace, under AFOSR Grant No. 274-66 and by the National Science Foundation.

† Supported in part by NASA Grant N6R 15-005-021 to Purdue University.

[1] G. D. Doolen, T. Kanki, and A. Tubis, Phys. Rev. **142**, 1072 (1966). The conventions and notation of this reference will be used in the present work.

[2] L. A. P. Balázs, Phys. Rev. **128**, 1935 (1962); **128**, 1939 (1962). For a list of references to calculations involving the method of Balázs, see E. Golowich, Phys. Rev. **139**, B158 (1965), footnotes 2–8.

[3] J. Hamilton and W. S. Woolcock, Rev. Mod. Phys. **35**, 737 (1963).

[4] M. H. Hull, Jr., and F. C. Lin, Phys. Rev. **139**, B630 (1965).

[5] L. D. Roper, R. M. Wright, and B. T. Feld, Phys. Rev. **138**, B190 (1965).

[6] P. Bareyre, C. Brickman, A. V. Stirling, and G. Villet, Phys. Letters **18**, 342 (1965).

[7] B. H. Bransden, P. J. O'Donnell, and R. G. Moorhouse, Phys. Letters **11**, 339 (1964).

[8] P. Auvil, C. Lovelace, A. Donnachie, and A. T. Lea, Phys. Letters **12**, 76 (1964).

[9] J. Cence, Phys. Letters **20**, 306 (1966).

[10] The analysis of Cence (Ref. 9) appears to be the only one in which the δ_{11} phase-shift maximum ($\approx40°$) is considerably smaller than 90°.